

Anthropogenic aerosols prolong fog lifetime in China

Jiannong Quan^{1,2*}, Yangang Liu^{2*}, Xingcan Jia^{1*}, Lin Liu¹, Youjun Dou¹,
Jinyuan Xin³, John H. Seinfeld⁴

¹Institute of Urban Meteorology, Chinese Meteorological Administration, Beijing, China

²Brookhaven National Laboratory, Environmental & Climate Sciences Department, New York, USA

³Institute of Atmospheric Physics, Chinese Academy of Sciences, Beijing, China

⁴California Institute of Technology, Pasadena, USA

* Corresponding Author: jnquan@ium.cn (J.Q.), lyg@bnl.gov (Y.L.) and xcjia@ium.cn (X.J.)

Abstract

Investigation of aerosol effects on fog with long-term measurements has generally focused on fog occurrence frequency and intensity; here we examine the effects on fog lifetime, fog formation, and fog dissipation. From analysis of 52 years (1960-2011) of data collected at 404 stations in China, it is found that fog lifetime exhibits a clear increasing trend with time, and the increased lifetime is mainly attributable to delayed fog dissipation. Increased aerosol levels and global warming affect fog lifetime in opposite ways; increased aerosol levels serve to prolong fog lifetime by primarily delaying fog dissipation, whereas warming decreases fog lifetime by primarily delaying fog formation. The overall aerosol effect on fog lifetime in China is shown to predominate, especially in the highly polluted region of Eastern China. The observational findings are confirmed by a suite of WRF-Chem simulations that reveal the influences of both increased aerosol levels and temperatures through a complex chain of interactions among microphysical, dynamical, thermodynamic, and radiative processes.

keywords: Fog lifetime; Aerosol; Global warming; Process interactions

1. Introduction

Fog can reduce visibility and affect traffic, air quality, human health, ecology, climate, and even cause catastrophic events (Gultepe *et al* 2007, Niu *et al* 2009, Johnstone and Dawson 2010). Aerosols play an important role in determining fog properties through acting as fog condensation nuclei. Moreover, at constant liquid water content and relative dispersion of the fog droplet size distribution, an increase in aerosol loading leads to an increase of fog droplet concentration, and a decrease of droplet size (Gultepe *et al* 2007, Quan *et al* 2011), enhancing light extinction (Kokkola *et al* 2003,

Elias *et al* 2015). Fog frequency of occurrence has been analyzed over 1000 stations worldwide (Johnstone and Dawson 2010, Quan *et al* 2011, Klemm and Lin 2016, Vautard *et al* 2009). For most stations, a significant decrease of fog occurrence over several decades has been identified (Klemm and Lin 2016, Vautard *et al* 2009), while a few stations show an increase or no detectable trends (Niu *et al* 2010; Quan *et al* 2011, Syed *et al* 2012). An increase of air temperature, through reduced relative humidity (RH), is a likely explanation for observed decreased fog frequency (Ding and Liu 2014), whereas increasing aerosol levels appear to increase fog frequency (Quan *et al* 2011, Vautard *et al* 2009; Gray *et al* 2019). Here we address the effects on fog lifetime of increased aerosol levels and surface temperature by analyzing long-term (1960-2011) observations of fog duration, clear sky visibility, and key meteorological variables (temperature, water vapor, and RH). We focus on China for which a relatively rich dataset is available and conduct a suite of WRF-Chem atmospheric simulations under varying conditions of aerosol level and temperature to evaluate the observational findings and elucidate the physical mechanisms underlying the observations.

2. Data and method

Long-term (1960-2011) fog observations were collected at 404 national meteorological stations in China (locations are shown in Fig.S1) for which inception and dissolution times of fog events were recorded by trained meteorological observers. Fog lifetime is calculated as the difference between the fog start and end times. Based on the China Meteorological Administration (CMA) criteria, a fog event is identified when the visibility is less than 1 km and RH exceeds 90%. In addition, observations of visibility and key meteorological variables (e.g., RH and temperature) were recorded 4 times a day, at 02:00, 08:00, 14:00 and 20:00, Beijing Standard Time (BST). Visibility was observed by trained meteorological professionals following the guidelines of the World Meteorological Organization (WMO, 2008). Visibility prior to 1980 was recorded in 10 classes; measurements after 1980 were recorded directly in kilometers. The conversion of the classified pre-1980 visibility data to kilometers is based on the work of Qin *et al.* (2010), and the relationship is provided in Table S1 in the Supporting Information (SI). To test the robustness of this transformation method, we transform the kilometer-based visibility measurements after the 1980s to the classification, and then back transform the classified data to kilometers with the same technique applied to the pre-1980s data. The result indicates that the recalculated visibilities agree generally with the observations, with $R^2=0.98$ and a small overestimation of 2.9-5.8% (4.3% on average) (Fig.S2). This measurement uncertainty related to the changes of the observational methods and data-processing methods may influence the visibility trend slightly. Further investigation with improved measurements is warranted. To minimize potential contamination on using visibility as a proxy for aerosol level, visibility data on the days when fog and/or precipitation (rain, snow) occurred were excluded in the analysis. Note that the RH effect on visibility is corrected by use of the method suggested by Rosenfeld *et al* (2007), and is used as a proxy for aerosol loading in view of much longer records of

1
2
3
4
5
6
7
8
9
10
11
12
13
14
15
16
17
18
19
20
21
22
23
24
25
26
27
28
29
30
31
32
33
34
35
36
37
38
39
40
41
42
43
44
45
46
47
48
49
50
51
52
53
54
55
56
57
58
59
60

visibility than direct measurements of aerosol levels. Wang *et al* (2009) show that the accuracy of aerosol optical depth (AOD) estimated from visibility measurements is comparable to that of both the Moderate Resolution Imaging Spectroradiometer (MODIS) and Multi-angle Imaging Spectro-Radiometer (MISR). Thus, increased aerosol loading is a likely factor underlying the trend of visibility degradation shown in Fig.1. Unfortunately, fog observations by CMA, including inception and dissolution time, were not continued after 2011. Aerosol loading has been largely decreasing in China over the last decade, which should result in a clear opposite (decreasing) signal in fog lifetime other conditions the same. Our study highlights the importance and need to conduct the observations of fog lifetime in the future. The WRF-Chem model is used to discern the interactions among aerosols, radiation, and fog (Grell and Devenyi 2002, Fast *et al* 2006, Chapman *et al* 2009). Detailed model description and experimental design are provided in the SI.

3. Results and Discussion

3.1 Trend analysis

Figure 1 shows the decadal variations of fog lifetime and visibility over the period of 1960 to 2011. The empirical Bayesian kriging (EBK) method is used in geo-statistical interpolation (Krivoruchko, 2011). A clear trend exists of increasing fog lifetime, especially in the highly polluted region of Eastern China (EC). Moreover, increased fog lifetime is primarily a result of delayed fog dissipation rather than hastened fog formation (Fig.2). On average, fog lifetime increased by 0.12 h per decade; fog dissipation was delayed by 0.17 h per decade; the start time delayed by 0.05 h per decade. Note that the correlation coefficient for fog start time ($R^2=0.28$) is smaller than those for fog end time ($R^2=0.72$) and fog duration ($R^2=0.52$), which supports the finding that the increased lifetime is mainly attributable to delayed fog dissipation. Moreover, variations of fog lifetime were not evenly distributed geographically; stations with clear prolonged fog lifetimes were located mainly in EC. Decadal variations of visibility and principal meteorological variables (temperature, water vapor, and RH) are further analyzed (Fig.S3). Visibility exhibited a clear decreasing trend over the period of 1960 to 2000, and stayed constant or even increased slightly after 2000. The increasing trend of temperature is associated with a slightly decreasing trend of RH (Fig.S3), because of the larger contribution of increased temperature to RH relative to that of increased water vapor (Liu *et al* 2018).

Aerosol levels and RH are the two dominant factors that affect fog lifetime (Table S2); high aerosol loading (low visibility) and/or a high RH prolong fog lifetime (Fig.S4, S5). Multivariable regression provides an empirical relationship between fog lifetime and visibility, temperature, and RH

$$Y = 0.026 - 0.11T + 0.041RH - 0.063Vis \quad (1)$$

where Y , T , RH and Vis denote the fog lifetime in h, temperature in $^{\circ}C$, relative humidity in % and visibility in km, respectively. The adjusted R^2 is 0.62 with a

significance level of $p < 0.001$. T , RH and Vis in equation (1) refer to the 14:00 data the day before the fog events occurred. To minimize the trend effect, the data were detrended (Wilks, 2006). From the trend of decreasing visibility, increasing temperature, and decreasing RH , increased aerosol levels are estimated to have prolonged fog lifetime by 0.09 h per decade, whereas global warming decreased fog lifetime by 0.04 h per decade (0.023 h per decade by increasing T and 0.018 h per decade by decreasing RH). We also conduct similar multiple regression over T , Vis and water vapor content, and found that increased aerosol levels and water vapor amount together with decreased T prolonged fog lifetime (see details in SI).

3.2 Regional Differences in China

As shown in Fig.1, the regions with high aerosol loadings are mainly located in EC. The mean visibility of the stations in EC was 17.7 km, while the mean visibility of stations in the other regions, including Western, Central and Northeast China (WCNC hereafter), was 30.9 km (Fig.3). In EC, fog lifetime exhibited a clear increasing trend at a rate of 0.15 h per decade, whereas fog lifetime slightly decreased in WCNC. Temperature increased in both EC and WCNC; but the increasing rate in EC was lower than that in WCNC, due likely to an aerosol cooling effect (Qian *et al* 2003, Ruckstuhl *et al* 2008). The increasing water vapor level in EC was lower than that in WCNC as well. As a result, RH showed similar decreasing trends in both EC and WCNC since saturated water vapor is negatively related to temperature. Thus, increased temperature and decreased RH in both EC and WCNC would presumably have led to a decrease in fog lifetime in both regions. However, the increasing trend of fog lifetime in EC is consistent with the opposing effect of aerosol level. The decreasing visibility in EC of 2.0 km per decade was 4 times higher than that in WCNC, whereas the increasing rate of temperature in EC (0.18°C per decade) was lower than that in WCNC (0.30°C per decade). The relative contributions of aerosol level and global warming, represented as $(\Delta Visibility / \Delta t) / (\Delta T / \Delta t)$, was $11.1 \text{ km } ^\circ\text{C}^{-1}$ in EC, exceeding $1.7 \text{ km } ^\circ\text{C}^{-1}$ in WCNC.

3.3 Model simulation

To investigate quantitatively the influence of aerosols on fog lifetime, sensitivity experiments were conducted with the WRF-Chem model for three aerosol emission scenarios: CLEAN (5% of base emissions), MEDIUM (50% of base emissions), POLLUT (base emissions). The results show that fog lifetime increased by 0.56 h as aerosols increase from CLEAN to MEDIUM scenarios, but levels off as aerosols further increase from MEDIUM to POLLUT scenarios (Fig.4). The aerosol-induced increase of fog lifetime stems primarily from delayed fog dissipation (0.59 h) rather than enhanced fog formation (-0.03 h) (Fig.4). An increase in aerosol concentration leads to increases in fog droplet number concentration (N_c) and in liquid water content (LWC), and a decrease in fog droplet effective radius (r_e) (Fig.S7). The increase of LWC with increasing aerosols is due likely to the combined effects of increased condensation, and reduced autoconversion and sedimentation (Maalick *et al.*, 2016; Stolaki *et al.*, 2015; see also Fig.S8 for attribution analysis of our simulation).

1
2
3
4
5
6
7
8
9
10
11
12
13
14
15
16
17
18
19
20
21
22
23
24
25
26
27
28
29
30
31
32
33
34
35
36
37
38
39
40
41
42
43
44
45
46
47
48
49
50
51
52
53
54
55
56
57
58
59
60

Furthermore, the changes in these microphysical properties, in turn, enhance emission of longwave radiation (Fig.S9), decrease atmospheric stability and enhance turbulence (Fig.S10), leading to a thicker fog layer and larger fog area during the period of fog formation and development (Fig.4, Fig.S10). During the dissipation period, decreased solar radiation at the surface under high aerosol levels (Fig.S9) delays fog dissipation. To examine the influence of temperature change on fog lifetime, sensitivity computations were performed with three scenarios under the same base emission intensity: base temperature (BASE), cooling by 1°C (T-1) and 2°C (T-2). As expected, warming decreases fog lifetime by delaying fog formation and accelerating fog dissipation (Fig.4, Fig.S11). It is noteworthy that unlike aerosols that preferentially affect fog dissipation rather than fog formation, temperature increase exerts more effect on fog formation than fog dissipation. We have also conducted similar sensitivity study on another fog event that occurred over the Northern China Plain on November 6-7, 2009. The results are similar and are shown in Fig.S12.

3.4 Analysis of physical mechanisms

Fog forms when the air becomes saturated. A lower initial RH requires a larger decrease of temperature to reach saturation state, and hence fog forms later, if the temperature decrease rate (TDR) is fixed. Hence, decreased RH under global warming (Fig.3) serves to delay fog formation. A heavy aerosol loading (low visibility) can also delay fog start time by decreasing TDR (Fig.S13). High aerosols warm the atmosphere which decreases TDR through absorbing longwave radiation and re-emitting it partially back towards the ground, acting like a thin low cloud (Zhou and Savijarvi 2014; Lubin et al., 2002). In the morning, the temperature increase rate is essential for understanding fog dissipation. Under high aerosol loading, more small fog droplets form (Gultepe et al., 2007; Quan et al., 2011), which enhance the extinction coefficient (Twomey, 1977), and hence slow down the rate of temperature rise (Fig.S12) and delay fog dissipation. Furthermore, an increase in aerosol levels increases liquid water content and turbulence, leading to a thicker fog layer and more extensive fog area (Fig.4), which also helps to delay fog dissipation.

4. Conclusions

On average, the effect of aerosol level on fog lifetime in China has led to a trend of a modest increase in fog lifetime over the period of 1960 to 2011, especially in the highly polluted region of Eastern China. Moreover, the increase of fog lifetime is shown to result mainly from delayed fog dissipation. At night, during fog formation, temperature drop is retarded under high aerosol loading due to aerosol longwave emission. In the development period, an increase in aerosol levels increases liquid water content and turbulence, leading to a thicker fog layer and more extensive fog area. In daytime, heavy fog with enhanced extinction of solar radiation diminishes lower atmosphere solar heating, slows down temperature rise, and delays fog dissipation. Overall, the retarding effect of aerosols on fog dissipation is stronger than that on fog formation, prolonging fog lifetime under high aerosol levels. On the large scale, global warming decreases RH, which delays fog formation, weakens fog

development by decreasing LWC, fog depth, and fog area, and accelerates fog dissipation.

It should be noted that the modeling study is based only on limited number of simulations of two cases. A more comprehensive modeling study is desirable in future to reduce possible model uncertainties and enhance physical understanding by using more ensemble members of different model settings (e.g., different initial and boundary conditions physical parameterizations) and observational cases.

226 **References**

- 227 Chapman E G, Gustafson W I, Jr. Barnard J C, Ghan S J, Pekour M S and Fast J D
228 2009 Coupling aerosol-cloud-radiative processes in the WRF-Chem model:
229 Investigating the radiative impact of large point sources *Atmos Chem Phys* 9
230 945-964
- 231 Ding Y H and Liu Y J 2014 Analysis of long-term variations of fog and haze in China
232 in recent 50 years and their relations with atmospheric humidity *Sci China Earth*
233 *Sci* 57 36-46
- 234 Elias T et al 2015 Enhanced extinction of visible radiation due to hydrated aerosols in
235 mist and fog *Atmos Chem Phys* 15 6605-6623
- 236 Fast J D et al 2006 Evolution of ozone, particulates, and aerosol direct radiative
237 forcing in the vicinity of Houston using a fully coupled
238 meteorology-chemistry-aerosol model *J Geophys Res* 111 D21305
- 239 Gray E, Gilardoni S, Baldocchi D, McDonald B C, and Goldstein A H 2019 Impact of
240 Air Pollution Controls on Radiation Fog Frequency in the Central Valley of
241 California *J Geophys Res* DOI: 10.1029/2018JD029419
- 242 Grell G A and Devenyi D 2002 A generalized approach to parameterizing convection
243 combining ensemble and data assimilation techniques *Geophys Res Lett* 29 1693
- 244 Gultepe I et al 2007 Fog research: A review of past achievements and future
245 perspectives *Pure Appl Geophys* 164 1121-1159
- 246 Johnstone J A and Dawson T E 2010 Climatic context and ecological implications of
247 summer fog decline in the coast redwood region *Proc Natl Acad Sci* 107
248 4533-4538
- 249 Klemm O and Lin N H 2016 What Causes Observed Fog Trends: Air Quality or
250 Climate Change? *Aerosol Air Qual Res* 16 1131-1142
- 251 Kokkola H, Romakkaniemi S and Laaksonen A 2003 On the formation of radiation
252 fogs under heavily polluted conditions *Atmos Chem Phys* 3 581-589
- 253 Krivoruchko K 2011 Spatial Statistical Data Analysis for GIS Users Redlands CA:
254 *Esri Press* 928 pp
- 255 Liu W J, Han Y X, Li J X, Tian X R and Liu Y G 2018 Factors affecting relative
256 humidity and its relationship with the long-term variation of fog-haze events in
257 the Yangtze River Delta *Atmos Environ* 193 242-250
- 258 Lubin D, Satheesh S K, McFarquar G and Heymsfield A J 2002 Longwave radiative
259 forcing of Indian Ocean tropospheric aerosol *J Geophys Res* 107 8004
- 260 Maalick Z, Kühn T, Korhonen H, Kokkola H, Laaksonen A and Romakkaniemi S
261 2016 Effect of aerosol concentration and absorbing aerosol on the radiation fog

- life cycle Atmospheric Environment 133 26-33
- Niu S, Lu C, Yu H, Zhao L and Lv J 2009 Fog research in China: An over-view *Adv Atmos Sci* 27 639-662
- Niu F, Li Z, Li C, Lee K H and Wang M 2010 Increase of wintertime fog in China: Potential impacts of weakening of the Eastern Asian monsoon circulation and increasing aerosol loading *J Geophys Res* 115 D00K20
- Qin S et al 2010 Long-term variation of aerosol optical depth in China based on meteorological horizontal visibility observations *Chin J Atmos Sci* 34 449-456
- Qian Y, Leung R L, Ghan S J and Giorgi F 2003 Regional climate effects of aerosols over China: modeling and observation *Tellus B* 55 914-934
- Quan J, Zhang Q, Liu J, Huang M and Jin H 2011 Analysis of the formation of fog and haze in North China Plain (NCP) *Atmos Chem Phys* 11 8205-8214
- Rosenfeld D et al 2007 Inverse relations between amounts of air pollution and orographic precipitation *Science* 315 1396-1398
- Ruckstuhl C et al 2008 Aerosol and cloud effects on solar brightening and the recent rapid warming *J Geophys Res* 35 L12708
- Stolaki S, Haeffelin M, Lac C, Dupont J C, Elias T and Masson V 2015 Influence of aerosols on the life cycle of a radiation fog event. A numerical and observational study *Atmos Res* 151 146-161
- Syed F S, Körnich H, Tjernström M 2012 On the fog variability over South Asia. *Clim Dyn* 39: 2993-3005
- Twomey S 1977 The influence of pollution on the shortwave albedo of clouds *J Atmos Sci* 34 1149-1152
- Vautard R, Yiou P, van Oldenborgh G J 2009 Decline of Fog, Mist and Haze in Europe over the Past 30 Years. *Nat Geosci* 2: 115-119
- Wang K, Dickinson R E and Liang S 2009 Clear Sky Visibility Has Decreased over Land Globally from 1973 to 2007 *Science* 323 1468-1470
- World Meteorological Organization 2008 WMO: Guide to meteorological instruments and methods of observation, WMO-No 8, 7th Edn., Geneva, Switzerland
- Wilks D S 2006 Statistical Methods in the Atmospheric Sciences 2nd Edition *Academic Press* San Diego
- Zhou Y and Savijärvi H 2014 The effect of aerosols on long wave radiation and global warming *Atmos Res* 135-136 102-111
- Acknowledgments** This research is supported by National Natural Science Foundation of China (41975181), and Chinese Key Projects in the National Science

1
2
3
4
5
6
7
8
9
10
11
12
13
14
15
16
17
18
19
20
21
22
23
24
25
26
27
28
29
30
31
32
33
34
35
36
37
38
39
40
41
42
43
44
45
46
47
48
49
50
51
52
53
54
55
56
57
58
59
60

and Technology (2017YFC0209604, 2018YFF0300101). Y.L. is supported by the US Department of Energy Atmospheric System Research (ASR) Program. The data were obtained from National Meteorological Information Center of China Meteorological Administration (<http://data.cma.cn/en>), which is open to the scientific community.

Additional information

The authors declare no competing financial interests.

306 **Figures**



Figure 1. Decadal variation of spatial distribution of fog lifetime (a, c, e, g, i) and visibility (b, d, f, h, j), and their trend (k, l) over the period of 1960 to 2011 in China. The visibility data are at 08:00 BST, in the absence of days of fog and/or precipitation. The red line plot (j) marks the border between Eastern China and remaining regions.

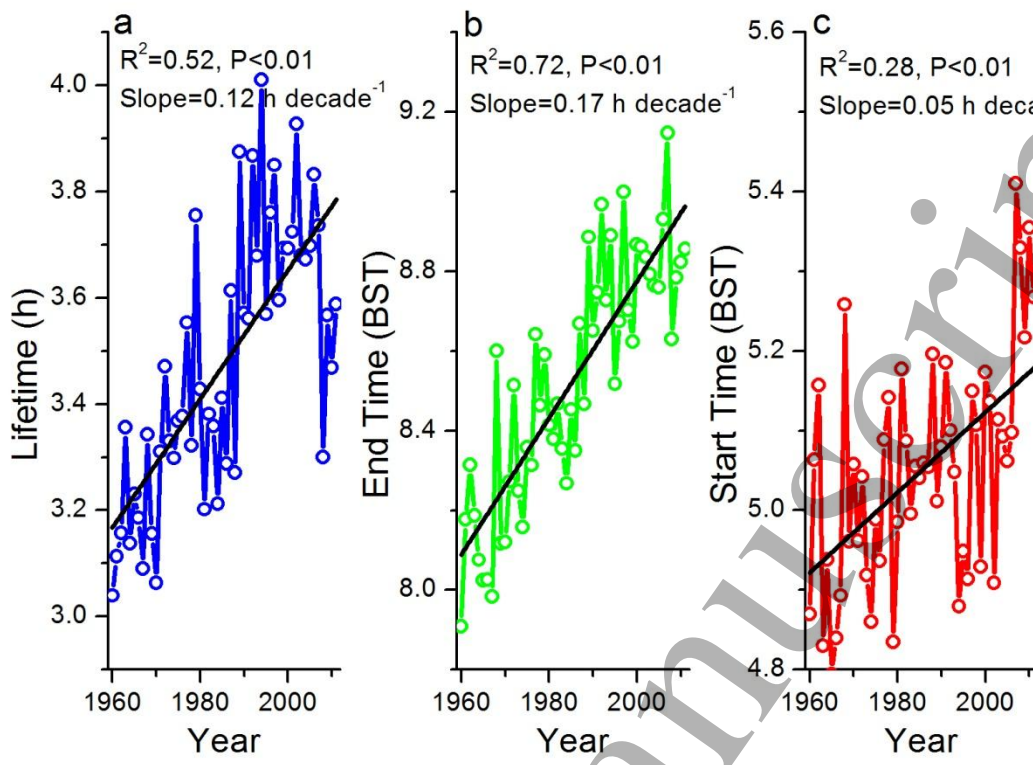


Figure 2. Inter-annual variation of fog duration (a), end time (b) and start time (c). Individual points are the spatial average of all 404 meteorological stations in China. Black lines represent linear regression.

318

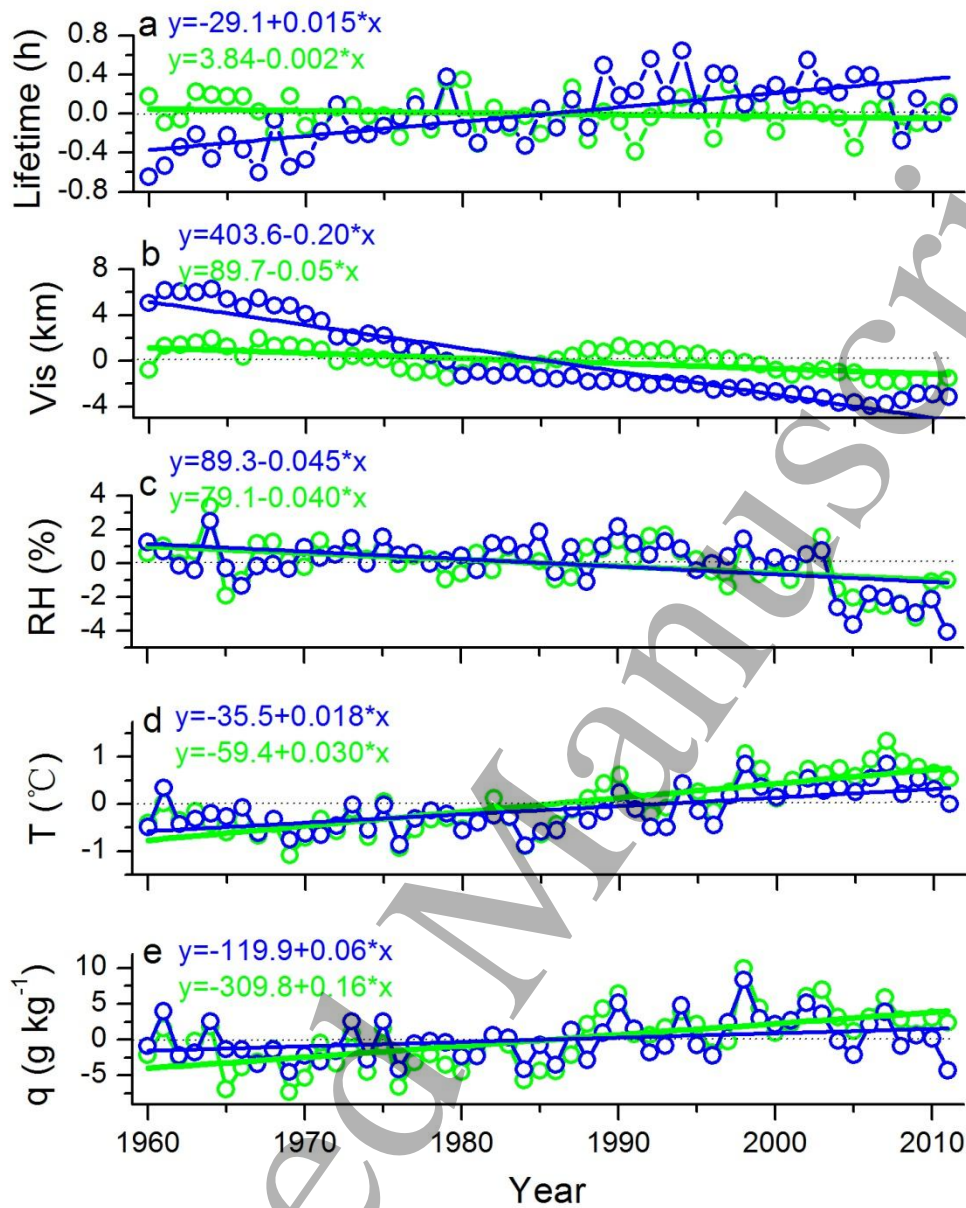


Figure 3. Comparison between EC (blue) and WCNC (green) regions of the anomalies of fog lifetime (a), visibility (b), RH (c), temperature (d), and water vapor mixing ratio (e). All the data, except fog lifetime, are at 08:00 BST. Blue and green lines represent the corresponding linear regressions, respectively.

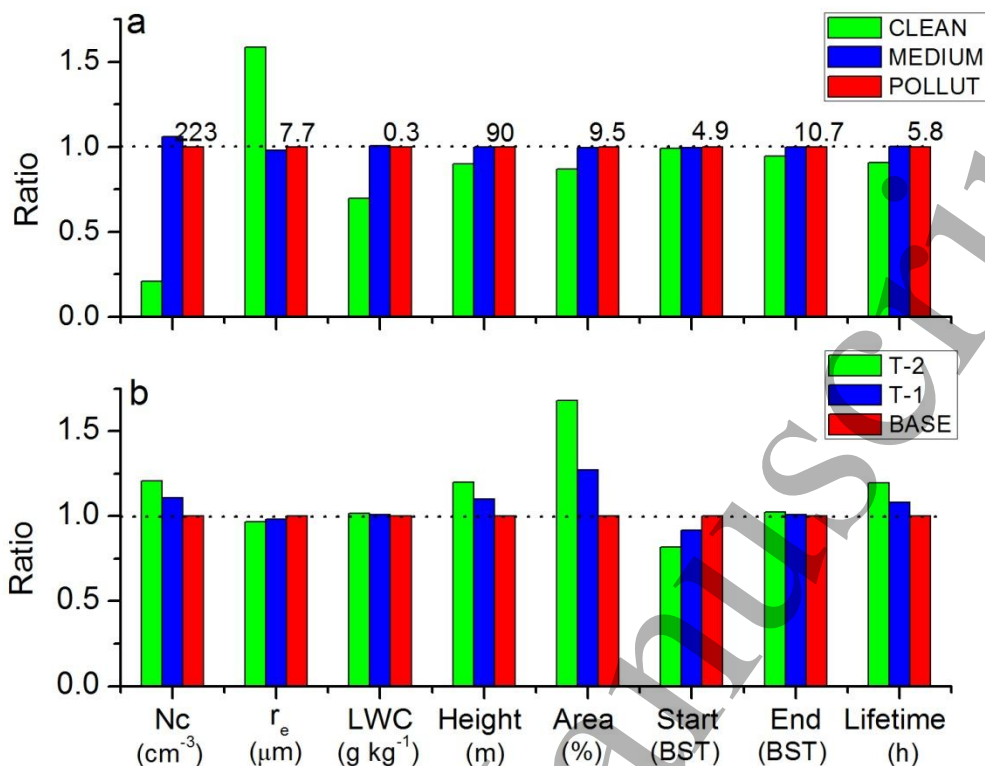


Figure 4. Comparison of key micro- and macro-physical fog properties under different aerosol levels (a) and temperatures (b). Three aerosol emission scenarios are CLEAN (5% of base emissions), MEDIUM (50% of base emissions), and POLLUT (base emissions) under the same base temperature. Three temperature scenarios are base temperature (BASE), cooling by 1 °C (T-1), and 2 °C (T-2) under the same base emission. The ratios are all relative to the base simulation, with the corresponding base properties values given on top of the red bar (POLLUT) of the upper panel. The fog area fraction is defined as the ratio of the number of fog grid cells to the total number of grid points; fog top is defined as the highest height of fog grid cells.